

# Development of New No-Flow Underfill Materials for Both Eutectic Sn-Pb Solder and a High Temperature Melting Lead-Free Solder

Haiying Li, Ashanti Johnson, and C. P. Wong, *Fellow, IEEE*

**Abstract**—In recent years, no-flow underfill technology has drawn more attention due to its potential cost-savings advantages over conventional underfill technology, and as a result several no-flow underfill materials have been developed and reported. However, most of these materials are not suitable for lead-free solder, such as Sn/Ag (m.p. 225 °C), Sn/Ag/Cu (m.p. 217 °C), applications that usually have higher melting temperatures than the eutectic Sn-Pb solder (m.p. 183 °C). Due to the increasing environmental concern, the demand for friendly lead-free solders has become an apparent trend. This paper demonstrates a study on two new formulas of no-flow underfill developed for lead-free solders with a melting point around 220 °C. As compared to the G25, a no-flow underfill material developed in our research group, which uses a solid metal chelate curing catalyst to match the reflow profile of eutectic Sn-Pb solder, these novel formulas employ a liquid curing catalyst thus provides ease in preparation of the no-flow underfill materials.

In this study, curing kinetics, glass transition temperature ( $T_g$ ), thermal expansion coefficient (TCE), storage modulus ( $E'$ ) and loss modulus ( $E''$ ) of these materials were studied with a differential scanning calorimetry (DSC), a thermo-mechanical analysis (TMA), and a dynamic-mechanical analysis (DMA), respectively. The pot-life in terms of viscosity of these materials was characterized with a stress rheometer. The adhesive strength of the materials on the surface of silicon chips were studied with a die-shear instrument. The influences of fluxing agents on the materials curing kinetics were studied with a DSC. The materials compatibility to the solder penetration and wetting on copper clad during solder reflow was investigated with both eutectic Sn-Pb and 95.9Sn/3.4Ag/0.7Cu solders on copper laminated FR-4 organic boards.

**Index Terms**—Electronic packaging, epoxy, eutectic Sn-Pb, flip-chip, fluxing agent, lead-free, no-flow, solder, underfill.

## I. INTRODUCTION

THE trend of developing high speed, high integration and low cost integrated circuits has led to the design of high-density and high input/output (I/O) area array packages, e.g., IBM's controlled collapse chip connection ( $C^4$ ) area array

bonding technology [1], [2]. As a result, direct chip attach (DCA) assemblies, primarily, flip-chip, and ball grid array, are becoming the mainstream in interconnect technology [3], [4]. In DCA, the pads of a chip or component are directly attached to the substrate, typically on a printed circuit board, as such, the interconnects are very short and solder balls are rigid. The size and cost of an individual component are thus reduced.

In this flip-chip interconnect technique, however, the mismatch in thermal expansion coefficient between an IC chip ( $\sim 2.5$ – $3.0$  ppm) and organic substrate ( $\sim 16$  ppm) brings more serious stress on IC chips and solder joints. Underfill technology thus has become very important to the success of flip-chip technology [5].

Polymeric materials are usually used as underfill encapsulants to physically reinforce the mechanical property of the solder joints. As a result, the fatigue life of the solder joints has been enhanced by ten to hundred folds.

Typical flip-chip underfill packaging process includes four major cascade steps:

- 1) chip placement and alignment;
- 2) solder bump re-flow and the formation of chip-substrate interconnection;
- 3) liquid underfill dispensing and capillary flowing into the chip-substrate gap of each flip-chip [6];
- 4) underfill curing.

Currently, more than 90% of encapsulated flip-chip packages are produced via this tedious process.

To address this issue, a process that combines solder bump fluxing and reflow, as well as underfill encapsulant curing steps has been proposed [7] and developed [8]–[11]. In this so-called no-flow process, the underfill material was dispensed on the substrate before the placement and alignment of an IC chip on the substrate. Then solder bump re-flowing and underfill material curing proceed simultaneously at an elevated reflow temperature. Therefore, the no-flow underfill must possess the following basic properties:

- 1) good fluxing ability;
- 2) minimal curing reaction occurs at the temperature below solder bump reflow temperature ( $\sim 190$ – $230^\circ\text{C}$ ) as to maintain a low viscosity in order to allow the solder to penetrate the underfill layer and form an interconnection with solder pad;
- 3) rapid curing takes place after the solder reflow;
- 4) good adhesion to passivation layer, chip, substrate, solder mask, and solder joints;

Manuscript received November 1, 2001; revised November 1, 2002. This work was recommended for publication by Associate Editor J. E. Morris upon evaluation of the reviewers' Comments. This work was supported by the NSF Packaging Research Center, Georgia Institute of Technology, Union Carbide Company, and Lindau Chemicals, Inc.

H. Li and C. P. Wong are with the School of Materials Science and Engineering, Packaging Research Center, Georgia Institute of Technology, Atlanta, GA 30332 USA (e-mail: cp.wong@mse.gatech.edu).

A. Johnson is with the School of Materials Science and Engineering, Packaging Research Center, Georgia Institute of Technology, Atlanta, GA 30332 USA and also with the Department of Chemistry, Morehouse College, Atlanta, GA 30314 USA.

Digital Object Identifier 10.1109/TCAPT.2003.815094

TABLE I  
FORMULATIONS OF NO-FLOW UNDERFILL MATERIALS

<b>Formula</b> <b>Component</b>	<b>Basic 1</b> <b>(mol.)</b>	<b>Basic 2</b> <b>(mol.)</b>	<b>Formula 1</b> <b>(mol.)</b>	<b>Formula 2</b> <b>(mol.)</b>	<b>Formula 3</b> <b>(mol.)</b>	<b>Formula 4</b> <b>(mol.)</b>	<b>Formula 5</b> <b>(mol.)</b>	<b>Formula 6</b> <b>(mol.)</b>
ERL-4221E	1		1	1			1.5	1.5
Bisphenol-A		1			1	1	0.5	0.5
HHMPA	1.6	1.6	1.6	1.6	1.6	1.6	3.2	3.2
Quinoline (catalyst)	0.03	0.03	0.03	0.03	0.03	0.03	0.06	0.06
CA-187			1.5wt. %	1.5wt. %	1.5wt. %	1.5wt. %	1.5wt. %	1.5wt. %
Heptanoic acid			0.225		0.225		0.45	
Lauric acid				0.225		0.225		0.45

- 5) low shrinkage of the material during curing;
- 6) proper CTE;
- 7) reasonable moduli to minimize the residual thermal stress resulted from the curing process and temperature cycling conditions.

Several no-flow underfill materials have been developed and reported in literature. Due to the increasing environmental concern, the demand for environmental friendly lead-free solders has become apparent. However, most of these materials are not suitable for lead-free solder applications because they usually require higher melting temperatures than eutectic Sn-Pb solders.

This paper demonstrated the study on two new formulations of no-flow underfill developed for both eutectic Sn-Pb and lead-free solders with melting points around 220 °C. As compared to G25, the first no-flow underfill material developed by our research group that uses a solid metal chelate curing catalyst to match the reflow profile of the eutectic Sn-Pb solder, these novel formulas employ a liquid curing catalyst which provides ease in preparation of the no-flow underfill materials and using organic acids as fluxing agents.

## II. EXPERIMENTAL

### A. Preparation of Underfill Formulations

In this study two new basic formulations were developed for the no-flow underfill process, and six samples were derived based on these two formulations (Table I). Both basic formulas contain an epoxy resin, a hardener and a curing catalyst. Formula Basic A employed 3, 4-epoxy cyclohexylmethyl-3, 4-epoxy cyclohexyl carboxylate (ERL4221E, Union Carbide), and formula Basic B used Poly (Bisphenol A-co-epichlorohydrin), glycidyl end-capped (MW377, Aldrich) as resin, both of these formulas use hexahydro-4-methylphthalic anhydride (HHMPA, Lindau Chemicals, Inc.) as the hardener, and quinoline (Aldrich), a liquid organic compound, as the catalyst. In addition to these resins, hardener and catalyst, the derived formulas also include a coupling agent and a fluxing agent selected from acrylic acid, heptanoic acid, lauric acid, palmitic acid, and valeric acid (all from Aldrich) for each sample. All components were added and mixed by stirring into a homogeneous mixture in a glass container. Silica powder (LE-05 surface reforming, size 5  $\mu\text{m}$ , Nippon Chemical Industrial Co., Ltd.) used in Formulas 5 and 6 for solder wetting test was added into the prepared formulas and mixed with ceramic milling medium in a wide mouth glass containers on a ball-miller for 4 h.

### B. Polymeric Sample Preparation and Curing Processes

All polymeric underfill samples were prepared in a similar fashion. About 4 g of a formulated material was poured into an aluminum pan of 37.5 mm in diameter, and then preheated at 100 °C for at least 30 min in a convective oven. Thereafter, all formulas were cured at 130 °C for 30 min, 150 °C for 1 h and 210 °C for another 30 min. Then these samples were allowed to slowly cool back to room temperature to avoid internal stress in these samples. The aluminum pan was peeled off and the sample was polished into a disk with two parallel surfaces (dimension  $\sim 5 \text{ mm } D \times 5 \text{ mm } H$ ) for further analyses.

### C. Measurement Methods

**Differential Scanning Calorimetry (DSC)** was carried out under a nitrogen atmosphere on DSC (TA Instruments Model 2920) with a sample of about 10 mg sealed in a hermetic aluminum pan. The kinetic curing profile was obtained by heating the formulated sample to a temperature around 300 °C with a heating rate at 5 °C/min. Thermogram of a cured sample was obtained by heating the sample to a temperature around 300 °C with a heating rate at 5 °C/min, while modulating  $\pm 1$  °C every minute.

**Thermomechanical Analysis (TMA)** was conducted on a TMA (Model 2940 by TA Instruments). A specimen for the TMA test was prepared by cutting the sample disk, as described previously, into a cubic of  $6 \times 6 \times 3 \text{ mm}$  in dimension using a diamond saw. Before running the TMA the specimen was treated at 250 °C and allowed to cool back to room temperature to remove the thermal history. The sample was heated from 25 °C to 250 °C at a rate of 5 °C/min and the thickness change versus temperature rise was monitored. Both onset and inflection points of thermal expansion were defined as TMA Tgs. A CTE below Tg ( $\alpha_1$ ) was measured either from 25 to 125 °C or to a temperature just below Tg (when Tg < 125 °C) and a CTE above Tg ( $\alpha_2$ ) was measured either from 175 to 250 °C or from a temperature just above Tg (when Tg > 175 °C).

**Dynamic Mechanical Analysis (DMA)** on dynamic modulus of cured materials was performed on a DMA (Model 2980 by TA Instruments). A specimen for DMA test was formulated and cured as described in A and B and cut into a  $30 \times 8 \times 3 \text{ mm}$  bar. The test was performed on a single cantilever under 1 Hz sinusoidal strain loading and the temperature was increased from room temperature to around 250 °C at a heating rate of

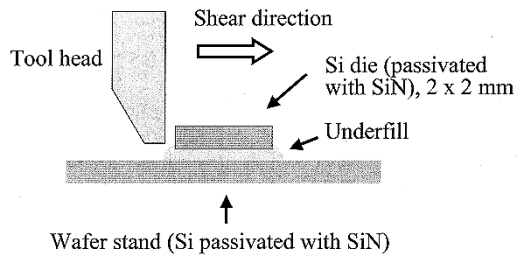


Fig. 1. Die shear test device and test vehicle.

5 °C/min. Storage modulus ( $E'$ ), loss modulus ( $E''$ ), and loss angle ( $\tan \delta$ ) were obtained. The temperatures at both onset and inflection points of storage modulus were defined as the DMA Tg.

**Thermogravimetric Analysis (TGA)** was conducted on a thermogravimetric analyzer (Model 2940 by TA Instruments). A cured sample of about 20 mg was placed in an open platinum pan and the sample was heated to about 400 °C with a heating rate of 10 °C/min in a nitrogen environment. The weight loss was monitored versus temperature and the decomposition temperature of the thermoset in nitrogen was then determined.

**Viscosity Measurement**—Viscosities of the formulated underfills were measured on a stress rheometer (Model AR1000N by TA Instruments). A cone-and-plate geometry was used and the operation was in flow mode so that the sample experienced a continuous shear rate or stress. The temperature of the sample was controlled by the stage plate. In this study the temperature ramped from 20 to 120 °C with a heating rate of 10 °C/min under a constant shear rate of 5.0 s<sup>-1</sup>.

**Moisture Absorption Study**—A specimen for this test was prepared exactly as for the DMA test. Two specimens of Basic 1 and Basic 2 were placed in an 85 °C/85%RH (relative humidity) chamber and the weight gain of each specimen was measured using a precious balance. The weight gain in percentage at different time intervals was defined as the moisture absorption of the material.

**Die Shear Test and Sample Preparation**—Silicon nitride passivated silicon dies of sizes 2 × 2 mm and 10 × 10 mm were used and the sample surfaces were cleaned prior to use according to a standard procedure [12]. Nine small dies were glued to one large die with the underfill formula, and glass beads of 75 μm in diameter in the amount of 0.5 weight% were added to the underfill formula to control the underfill thickness. The amount of underfill applied under a small die was carefully controlled to avoid the formation of a fillet. The underfill formulas were then cured as described above. Die shear test was performed on a die bond tester (Model 550–100 K by Royce Instruments) and the die shear strength is reported in MPa (Fig. 1).

**Study of Solder Wetting on Copper**—Copper foil-laminated copper clad on FR-4 board, eutectic 63Sn/37Pb solder balls (m.p. 183 °C) and 95.9Sn/3.4Ag/0.7Cu solder balls (m.p. 217 °C) (both from Indium Corp.) were used as received. To begin with this test, the preservative copper foil was peeled off and an uncured noflow material was immediately dispensed on the fresh copper clad before several solder balls were placed on the uncured material layer. This test assembly was then exposed

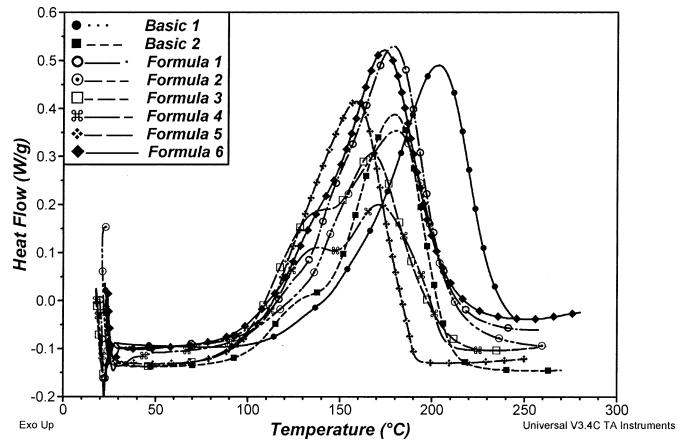


Fig. 2. DSC diagrams of curing kinetics of formulas at 5 °C/min heating rate.

to the reflow temperature by going through a five-heating-zone reflow oven. The wetting of solder melt on copper surface was examined with and without an optical microscope.

### III. RESULTS AND DISCUSSION

#### A. Development of Underfill Formulations

Two new underfill formulas, namely Basic 1 and Basic 2, were developed. Basic 1 uses 3, 4-epoxy cyclohexyl-methyl-3, 4-epoxy cyclohexyl carboxylate (ERL4221E, Union carbide), and Basic 2 uses Poly (Bisphenol A-co-epichlorohydrin), glycidyl end-capped (MW377) as resins, while both use HHMPA as the hardener and quinoline as their catalyst which provided a fast and easy mixing process and also more importantly, high curing temperature latency.

The curing profiles of these two materials obtained on a DSC with a curing rate of 5 °C/min are shown in Fig. 2. The exothermal peak temperatures of Basic 1 and Basic 2 are 203 °C and 179 °C, respectively. These peak temperatures are comparable to those of materials developed by our group [8]–[11]. The 203 °C curing peak temperature of Basic 1 made it possible to be used for lead-free solders that have melting points around 220 °C. Since these two formulas are different only in using different epoxy compounds, the difference in exothermal peak temperatures indicates that the steric hindrance of epoxy compounds possibly controlled the initiation of the curing process.

Organic acids have been widely used as fluxing agents in flip-chip process. In a no-flow process, the fluxing agent is added to the underfill formulas as one of the components to flux the solders and substrate pads during the combined solder reflow and epoxy curing step. However, it is well known that both base and acid can act as the catalysts to initiate the curing of an epoxide, and thus whether the acid accelerate the curing behavior of the materials is a concern. To study the influence of a fluxing agent on curing process of a no-flow underfill formula, the curing profiles of Basic 1 containing different fluxing agents were collected on a DSC. As compared to the curing profile of Basic 1 which contains no fluxing agent, both heptanoic acid and lauric acid slightly moved the curing profile about 23 °C lower, while acrylic acid decreased the

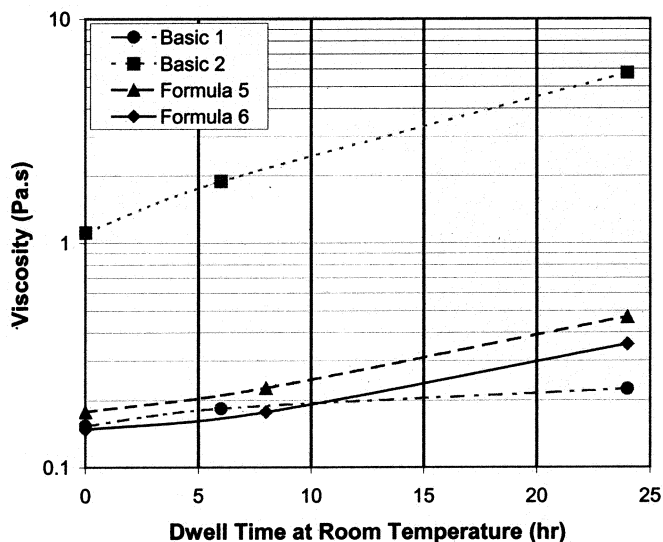


Fig. 3. Viscosity change at constant shear rate of  $5 \text{ s}^{-1}$  for Basics 1 and 2, and Formulas 5 and 6 after exposed to room temperature for different dwell time.

curing peak about  $35^\circ\text{C}$ . On the other hand, Basic 1 containing palmitic acid and valeric acid showed reduced thermal integrals, which indicate incomplete curing processes. Based on this result, heptanoic acid and lauric acid were chosen and used as the fluxing agents of six formulas derived from formulas Basic 1 and Basic 2 (Table I). Curing profile on a DSC of Basic 1, Basic 2 and Formulas containing heptanoic acid and lauric acid are shown in Fig. 2. Formulas 1 and 2 (both based on Basic 1 and containing heptanoic acid and lauric acid, respectively) showed curing peaks around  $180^\circ\text{C}$  as compared to  $203^\circ\text{C}$  of that of Basic 1, whereas Formulas 3 and 4 (both based on Basic 2 and containing heptanoic acid and lauric acid, respectively) showed curing peaks around  $170^\circ\text{C}$  as compared to  $179^\circ\text{C}$  of that of Basic 2.

Coupling agents can dramatically enhance the adhesion strength of underfill materials to the surface of a silicon chip. CA-187, an epoxy-silane coupling agent, was found to provide an improvement on adhesion strength, and thus was used in our formulas [13].

Cycloaliphatic epoxy resins have low viscosity before curing but usually show poor toughness. On the other hand, bisphenol A epoxy resins have higher viscosity before curing but provide good toughness. Formulas 5 and 6 were thus prepared by mixing cycloaliphatic epoxy, ERL-4221 and bisphenol A to obtain enhanced toughness while maintaining the viscosity at an acceptable level.

The rheological behaviors and the pot-life of Basics 1 and 2, and Formulas 5 and 6 were studied using a cone and plate rheometer. The viscosity changes of the uncured materials versus temperature at a constant shear rate of  $5 \text{ s}^{-1}$  were observed and recorded. The viscosity change versus time of these four formulas at room temperature is shown in Fig. 3. The viscosity of Basic 1 was determined to be  $0.19 \text{ Pa.s}$  right after the preparation, but increased to  $0.24$ ,  $0.29$ , and  $0.64 \text{ Pa.s}$ , after stored at room temperature for 6, 24, and 48 h, respectively. The corresponding data for Basic 2 were  $1.65$ ,  $2.9$ ,  $9.2$ , and  $34 \text{ Pa.s}$ , respectively. Since the pot-life of an underfill material

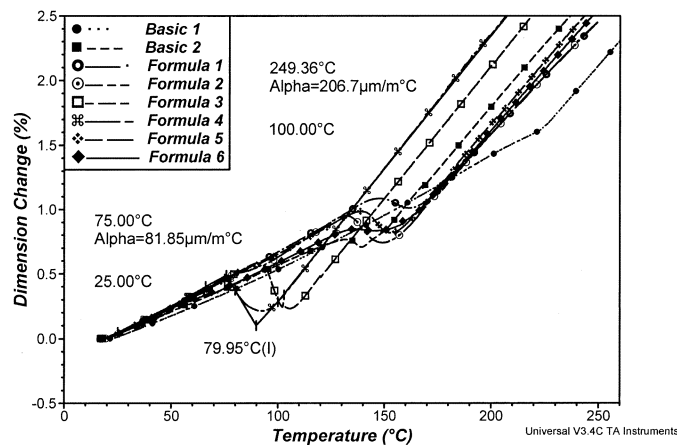


Fig. 4. TMA diagrams of eight cured materials.

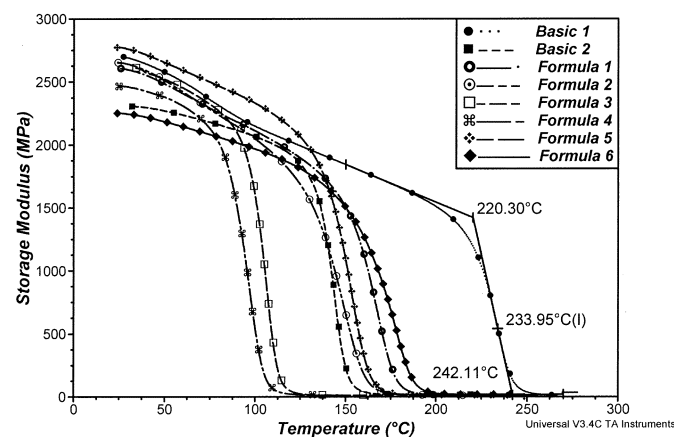


Fig. 5. DMA diagrams of eight cured materials.

is usually defined as the time that the initial viscosity doubles the pot-life data of Basics 1 and 2 were determined to be 32 h and 9.33 h, respectively. Both are longer than one shift (8 h) and thus they would be acceptable materials by most users. The viscosity data of Formulas 5 and 6 were almost the same as that of Basic 1 initially but they increased to a higher level than Basic 1 at the end the pot-life of Formulas 5 and 6 were estimated to be 18 h and 20 h, respectively.

### B. Thermal Properties

The glass transition temperatures ( $T_g$ ) of eight fully cured materials were observed on a TMA (Fig. 4) and a DMA (Fig. 5), and listed in Table II. The cured Basic 1 showed its  $T_g$  around  $223$ – $234^\circ\text{C}$ , and the cured Basic 2 gave its  $T_g$  around  $130$ – $144^\circ\text{C}$ .  $T_g$ s of Formulas 1 and 2, both based on Basic 1, were  $149$ – $167^\circ\text{C}$  and  $133$ – $149^\circ\text{C}$ , and  $T_g$ s of Formulas 3 and 4, both based on Basic 2, were  $94$ – $107^\circ\text{C}$  and  $78$ – $97^\circ\text{C}$ , respectively.  $T_g$ s of Formula 1 and 2 were above  $70$  to  $90^\circ\text{C}$  lower than those of their corresponding basic formula, Basic 1, and  $T_g$ s of Formula 3 and 4 were above  $36$  to  $52^\circ\text{C}$  lower than those of their corresponding basic formula, Basic 2. Also noted is the formulas containing lauric acid showed lower  $T_g$ 's than the corresponding heptanoic acid containing formulas. This is probably due to the fact that these fluxing agents may act as plasticizers or catalysts that decreased the molecular weight

TABLE II  
CTE AND Tg DATA INTERPRETED FROM TMA AND DMA DIAGRAMS

Formula	TMA Data				DMA Data	
	CTE, $\alpha 1$ ppm/ $^{\circ}$ C	CTE, $\alpha 2$ ppm/ $^{\circ}$ C	Tg, $^{\circ}$ C (onset)	Tg, $^{\circ}$ C (inflection)	Tg, $^{\circ}$ C (onset)	Tg, $^{\circ}$ C (inflection)
Basic 1	83.1	230.1	223.1	223.1	220.3	234.0
Basic 2	70.6	189.9	129.5	135.9	134.0	144.0
Formula 1	85.0	175.3	148.6	155.5	152.6	167.0
Formula 2	83.2	176.6	133.9	139.3	132.6	148.9
Formula 3	83.0	205.7	93.8	97.5	96.9	106.5
Formula 4	81.9	206.7	78.0	80.0	85.3	96.8
Formula 5	83.4	195.5	141.5	144.8	138.9	153.1
Formula 6	75.7	185.1	132.2	145.2	157.3	177.9

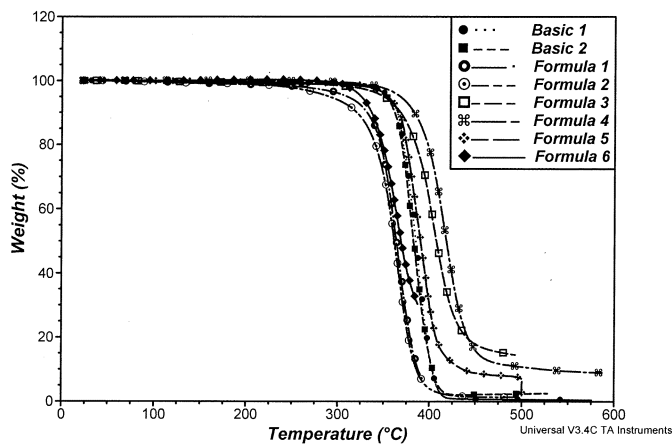


Fig. 6. TGA diagrams of cured eight materials.

of resins, or both. Since lauric acid lowered the Tg more than heptanoic acid which has a shorter chain than the former, the plasticizing effect probably was the dominating mechanism. Both Formulas 5 and 6 showed single Tgs which indicated that the two diepoxides were polymerized into the copolymer in an alternate way.

The coefficients of thermal expansion (CTE) of cured materials were determined by TMA as shown in Fig. 4 and Table II. All six formulas showed  $\alpha 1$  in the range of 71–85 ppm/ $^{\circ}$ C and  $\alpha 2$  in the range of 175–230 ppm/ $^{\circ}$ C. As compared to Basic 1, both Formulas 1 and 2 showed similar  $\alpha 1$  values, and about 55 ppm/ $^{\circ}$ C decreased  $\alpha 2$  values. Whereas both Formulas 3 and 4 showed about 12 ppm/ $^{\circ}$ C increased  $\alpha 1$  and 16 ppm/ $^{\circ}$ C increased  $\alpha 2$  as compared to those of Basic 2.

The thermodynamic behaviors of the eight cured formulas were obtained from DMA (Fig. 5). The storage modulus at 30  $^{\circ}$ C of the cured Basics 1 and 2 were 2.7 GPa and 2.3 GPa, respectively. When the temperature increased above 100  $^{\circ}$ C, the storage modulus of cured Basics 1 dropped to the same level as that of Basic 2. The storage modulus of all other formulas basically filled between those of Basics 1 and 2.

The thermal stability of the eight materials was studied with a TGA. The TGA diagrams are shown in Fig. 6. All the cured formulas were quite thermally stable until 300  $^{\circ}$ C where Formulas 1 and 2 started to decompose. At 350  $^{\circ}$ C all the rest formulas started their decomposition and then all materials quickly lost all the weight when the temperature rose to 420  $^{\circ}$ C.

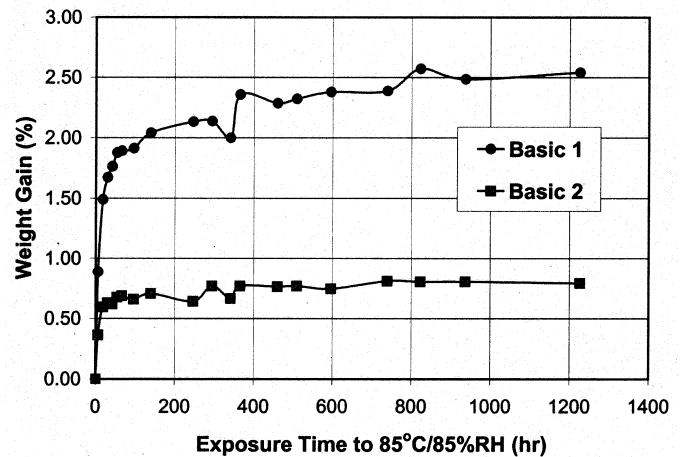


Fig. 7. Moisture absorption kinetics under 85  $^{\circ}$ C/85%RH condition of cured Basics 1 and 2.

### C. Moisture Resistance

Fig. 7 shows that the moisture up-take of cured Basics 1 and 2. The cured Basic 1 absorbed moisture faster and more than the cured Basic 2 through the whole study process. At saturation, their moisture uptakes are about 2.5wt% and 0.8wt%, respectively. The relatively high moisture absorption of cured Basic 1 is understandable since the cyclophatic epoxy resin, ERL-4221E, it based contains hydrophilic carbonyl group, while Bisphenol A that Basic 2 based does not.

### D. Adhesion

The die shear test result given in Fig. 8 indicates that both Basic 1 and 2 exhibited good adhesive strength to the SiN passivation layer. However, upon being exposed to 85  $^{\circ}$ C and 85% relative humidity for 500 h, adhesion stress of both formulas dropped more than 70%. The adhesion strength test on Formulas 1 through 6 showed that the addition of coupling agent, CA-187, dramatically enhanced the adhesion strength of aged materials even though it did not influence the adhesion strength of materials before aging. The addition of organic acids as fluxing agents exhibited different result in adhesion strength after aging. Generally, the heptanoic acid compromised the adhesion enhancement of coupling agent as compared to lauric acid with the exception on the case of Formulas 3 and 4.

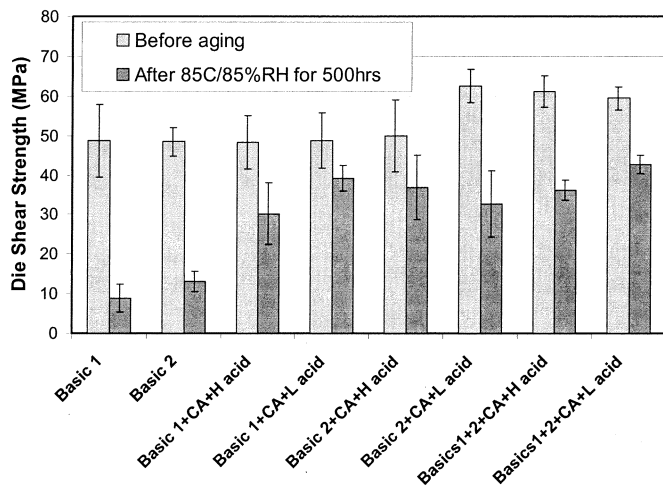


Fig. 8. Die shear strength of the eight materials.

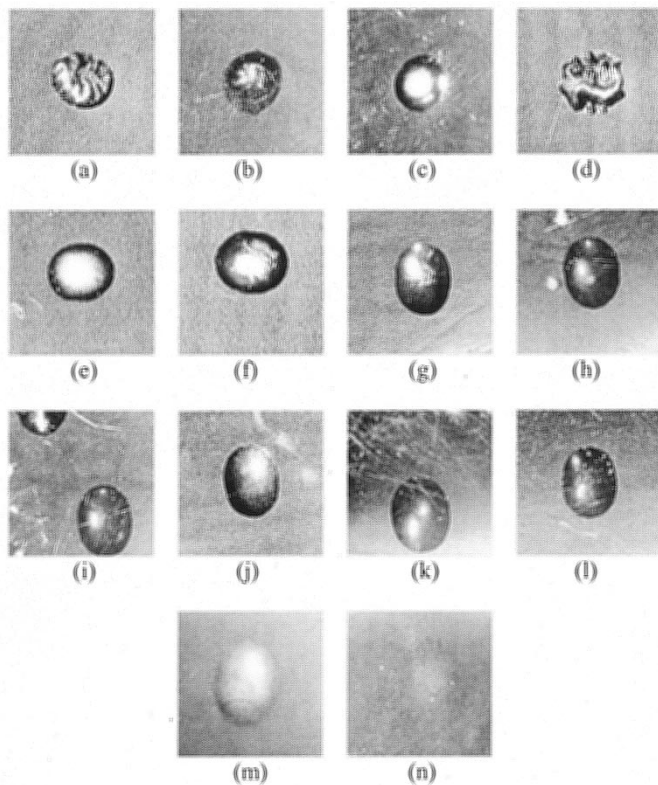


Fig. 9. Photographs of solder wetting on copper clad: (a) to (f) 95.9Sn/3.4Ag/0.7Cu solders on Formulas 1 to 6, respectively; (g) to (l) eutectic Sn-Pb solders on Formulas 1 to 6, respectively; (m) and (n) eutectic Sn-Pb solders on Formulas 5 and 6 with 20wt%  $\text{SiO}_2$  filler of size  $5 \mu\text{m}$ .

#### E. Compatibility to Solder Wetting on Copper

The test of solder wetting on copper was used to examine the ability of an underfill material to allow the solder to penetrate and wet the metal pads during the reflow process. Photographs in Fig. 9 show that Formulas 1 to 6 allowed both eutectic Sn-Pb and lead-free Sn/Ag/Cu solders to wet on the copper clad after the reflow process. As comparison, the wetting effect of Sn/Ag/Cu solder is not as good as that of eutectic Sn-Pb solder due to its low wetting ability on copper surface, an intrinsic property of Sn/Ag/Cu alloys [14], [15]—they usually exhibit

higher surface tension than Sn-Pb solder. Formulas 5 and 6 filled with 20wt% of  $\text{SiO}_2$  powders with a average particle size of  $5 \mu\text{m}$  also exhibited good solder wetting on copper surface. However, with higher  $\text{SiO}_2$  filler loadings Formulas 5 and 6 failed to give solder wetting on the same condition.

#### IV. CONCLUSION

Eight new underfill formulas for no-flow process were developed and characterized. These materials exhibited curing property that allow a fully curing within 1.5 h at  $160\text{--}200^\circ\text{C}$  while provide compatibility to both eutectic Sn-Pb and Sn/Ag/Cu solder reflow processes, and two organic acids could be used as fluxing agents for these no-flow formulations. The cured materials showed very good thermomechanical properties and excellent thermal stability. The cured formula, Basic 2, exhibited a relatively low moisture uptake. The solder wetting test indicated that Formulas 1 to 6 allowed both eutectic Sn-Pb and lead-free solder to wet on copper surface and Formulas 5 and 6 containing 20wt% of  $\text{SiO}_2$  fillers of  $5 \mu\text{m}$  particle size also exhibited good solder wetting effect.

#### REFERENCES

- [1] R. Marrs, "Trends in IC packaging," *Electron. Packag. Prod.*, pp. 24–30, Aug. 1996.
- [2] R. R. Tummala, E. J. Rymaszewski, and A. Klopfenstein, Eds., *Microelectronics Packaging Handbook*, 2nd ed. New York: Chapman & Hall, 1997.
- [3] F. Nakano, T. Soga, and S. Amagi, "Resin insertion effect on thermal cycle resistivity of flip-chip mounted LSI devices," in *Proc. Int. Soc. Hybrid Microelectron. Conf.*, 1987, p. 536.
- [4] D. Suryanayana, R. Hsiao, T. P. Gall, and J. M. McCreary, "Flip-chip solder bump fatigue life enhanced by polymer encapsulation," in *Proc. 40th IEEE Electron. Comp. Technol. Conf.*, 1990, p. 338.
- [5] D. Suryanayana and D. S. Farquhar, "Underfill encapsulant for flip-chip applications," in *Chip on Board*, J. H. Lau, Ed. New York: Van Nostrand Reinhold, 1994, pp. 504–531.
- [6] L. Nguyen *et al.*, "High performance underfills development-materials, process, and reliability," in *Proc. IEEE Int. Symp., Polym. Electron. Packag.*, Oct. 1997, p. 300.
- [7] C. P. Wong and D. F. Baldwin, "No-Flow underfill for flip-chip packages," U.S. patent pending, Apr. 1996.
- [8] C. P. Wong and S. H. Shi, "No-flow underfill of epoxy resin, anhydride, fluxing agent and surfactant," U.S. patent 6 180 696, Jan. 2001.
- [9] S. H. Shi and C. P. Wong, "Study of the fluxing agent effects on the properties of no-flow underfill materials for flip-chip applications," *IEEE Trans. Comp., Packag., Manufact. Technol. A*, vol. 22, pp. 141–151, June 1999.
- [10] C. P. Wong, S. H. Shi, and G. Jefferson, "High performance no-flow underfills for low-cost flip-chip applications: material characterization," *IEEE Trans. Comp., Packag., Manufact. Technol. A*, vol. 21, pp. 450–458, Sept. 1998.
- [11] S. H. Shi and C. P. Wong, "Recent advances in the development of no-flow underfill encapsulants—a practical approach toward the actual manufacturing application," *IEEE Trans. Comp., Packag., Manufact. Technol. C*, vol. 22, pp. 331–339, Oct. 1999.
- [12] M. B. Vincent, L. Meyers, and C. P. Wong, "Enhancement of underfill adhesion to die and substrate by use of silane additives," in *Proc. Int. Symp. Adv. Packag. Mater: Process, Properties Interfaces*, Braselton, GA, 1998, p. 49.
- [13] S. Luo and C. P. Wong, "Influence of temperature and humidity on adhesion of underfills for flip chip packaging," in *Proc. 51th IEEE Electron. Comp. Technol. Conf.*, 2001, p. 155.
- [14] N. C. Lee, "Lead-free soldering—Where the world is going," *Adv. Microelectron.*, vol. 26, no. 5, p. 29, 1999.
- [15] B. Huang and N. C. Lee, "Prospect of lead free alternatives for reflow soldering," in *Proc. SPIE—Int. Soc. Opt. Eng.*, vol. 39, 1999, p. 771.



**Haiying Li** received the B.S. degree in polymer science and engineering from the Beijing Institute of Chemical Technology, Beijing, China, in 1983, the M.S. degree in chemistry from Clark College, Atlanta, GA, in 1996, and is currently pursuing the Ph.D. degree at the Georgia Institute of Technology, Atlanta.

After receiving the B.S. degree, he served as a Polymer Engineer in industry for ten years. He has authored and co-authored 16 journal and proceedings articles and three U.S. patents.

Mr. Li received the Third Award of the Light Industry Ministry of China for the Progress in Science and Technology in 1989 and 1991 and was nominated as one of the finalists for ICI Student Award in Applied Polymer Science in 2000. He is a member of the American Chemical Society.



**C. P. Wong** (SM'87-F'92) received the B.S. degree in chemistry from Purdue University, West Lafayette, IN, and the Ph.D. degree in organic/inorganic chemistry from Pennsylvania State University, University Park.

After his doctoral study, he was awarded two years as a Postdoctoral Scholar at Stanford University, Stanford, CA. He joined AT&T Bell Laboratories, in 1977 as a Member of Technical Staff. He was elected an AT&T Bell Laboratories Fellow in 1992. He is a Regents Professor with the School of Materials

Science and Engineering and a Research Director at the NSF-funded Packaging Research Center, Georgia Institute of Technology, Atlanta. He holds over 40 U.S. patents, numerous international patents, has published over 400 technical papers and presented 300 key-notes and presentations in the related area. His research interests lie in the fields of polymeric materials, high T<sub>c</sub> ceramics, materials reaction mechanism, IC encapsulation, in particular, hermetic equivalent plastic packaging, electronic manufacturing packaging processes, interfacial adhesions, PWB, SMT assembly, and components reliability.

Dr. Wong received the AT&T Bell Laboratories Distinguished Technical Staff Award in 1987, the AT&T Bell Labs Fellow Award in 1992, the IEEE Components, Packaging and Manufacturing Technology (CPMT) Society Outstanding and Best Paper Awards in 1990, 1991, 1994, 1996, and 1998, the IEEE Technical Activities Board Distinguished Award in 1994, the 1995 IEEE CPMT Society's Outstanding Sustained Technical Contribution Award, the 1999 Georgia Tech's Outstanding Faculty Research Program Development Award, the 1999 NSF-Packaging Research Center Faculty of the Year Award, the Georgia Tech Sigma Xi Faculty Best Research Paper Award, the University Press (London, UK) Award of Excellence, and was elected a member of the National Academy of Engineering in 2000. He served as the Technical Vice President (1990 and 1991), and the President (1992 and 1993) of the IEEE-CPMT Society.

**Ashanti Johnson** received the B.S. degree in chemistry from Morehouse College, Atlanta, GA, in 2002.

He was an Intern at the Georgia Institute of Technology, Atlanta, Summer 2001.